Simplification strategies for the qutrit ZX-calculus

Alex Townsend-Teague [1] and Konstantinos Meichanetzidis [1,2]

[1] University of Oxford
[2] Cambridge Quantum Computing Ltd.

Abstract. The ZX-calculus is a graphical language for suitably represented tensor networks - namely ZX-diagrams. Calculations are done by transforming ZX-diagrams with rewrite rules. The ZX-calculus has found applications in reasoning about quantum circuits, condensed matter systems, quantum algorithms, surface code surgery, and recently about counting problems. A key notion of such results is the stabiliser fragment of the ZX-calculus, a subfamily of ZX-diagrams for which rewriting can be done efficiently in terms of derived simplifying rewrites. In quantum computation with qubits or of Boolean counting problems, one employs the qubit ZX-calculus. Recently, higher dimensional qudits have become more prominent in quantum computing, and there are counting problem families whose complexity depends on the dimension. The main contribution of this work is the derivation of *efficient* rewrite strategies for the stabiliser fragment of the *qutrit* ZX-calculus. This constitutes a first non-trivial step towards simplification of qutrit quantum circuits. Finally, we reinterpret known complexity-theoretic results about evaluating the Jones polynomial, an important link-invariant, and counting graph colourings.
Eligible for the best student paper award.

1   Introduction

The ZX-calculus originates in quantum foundations [6,24]. It is a graphical language that allows for reasoning about ZX-diagrams, which are interpreted as tensor networks over a (semi)ring [23]. The calculus is defined by a set of rewrite rules that transforming the diagrams. Note that the set of rewrite rules *depends* on the (semi)ring over which they are interpreted. Importantly, ZX rewrites are sound and complete.

In the context of quantum computing, the Gottesman-Knill theorem states that stabilizer quantum circuits can be simulated *efficiently* on classical computers [1], where by simulation here we mean the *exact* computation of quantum probability amplitudes. An alternative proof of the Gottesman-Knill theorem for qubits has been obtained graphically in terms of the qubit ZX-calculus. Stabilizer circuits can be expressed by the *stabilizer* fragment of the ZX-calculus, and stabilizer ZX-diagrams can be rewritten efficiently in terms of derived rewrite strategies [9]. Moreover, these simplifying rewrites can be viewed as theorems

that are useful for simplifying or simulating universal quantum circuits, not just stabilizer circuits. The key rewrite rules that enable the efficient rewriting of qubit stabilizer ZX-diagrams are called *local complementation* and *pivot*, the latter being a composition of three of the former [9]. In this work, we recall the *qutrit* version of local complementation [22] and derive the corresponding pivot rule. We then derive simplification strategies which allow for the *efficient* rewriting of qutrit stabilizer ZX-diagrams, the core result of this work.

Interestingly, though the motivation for studying ZX diagrams stems from quantum computation, they have broader applicability as they can express arbitrary linear maps; every quantum circuit is a ZX-diagram but not vice versa. A plethora of hard problems in physics and computer science regard interacting many-body multi-state systems - both classical and quantum - and reduce to *exactly* computing a single scalar. These range from quantum amplitudes, partition functions in classical statistical mechanics, counting problems, probabilistic inference, and many more. Problem instances can be encoded as closed tensor networks over an appropriate (semi)ring. The scalar can be evaluated by *full tensor contraction*, which in general is #P-hard [7], and finding the optimal contraction path for a general tensor network is NP-hard.

If a scalar of interest is expressed as a closed ZX-diagram, one can rewrite the diagram by applying rewrite rules; one's goal is then to perform *full diagram simplification* in order to compute the desired scalar. Again, simplifying arbitrary closed ZX-diagrams is #P-hard and finding the optimal rewrite strategy is NP-hard. Note that given an arbitrary tensor network, one can attempt to invent rewrite rules by inspecting the contents of the tensors and performing linear-algebra operations [13].

ZX-diagrams have been leveraged to study the complexity of boolean satisfiability (SAT) and model counting (#SAT) [5]. Model counting entails computing the number of satisfying assignments to a boolean formula, and this number can be expressed as a closed diagram. Specifically, one finds that in the case of XOR-SAT and #XORSAT, known to be tractable, the corresponding ZX-diagrams representing the problems exactly correspond to qubit stabilizer diagrams. Going further, the ZH calculus [3], an equivalent language to ZX, can be imported to make graphically obvious why 2SAT is in P but #2SAT is #P-complete, whereas 3SAT and #3SAT are both hard. The key realisation is that the decision problem is in fact a counting problem but where the diagram is interpreted over the Boolean semiring. Then the *rewrite rules change accordingly* and quickly imply the above result by allowing efficient simplification strategies.

In the spirit of [5], we treat the ZX-calculus as a library of rewrite rules, from which we import the appropriate tools for the job depending on the occasion. Here we present two case studies: evaluating the Jones polynomial at lattice roots of unity, and graph colouring. Both of these problem families reduce to evaluating closed tensor networks and show a transition in complexity at a particular dimension, below which the tensor network corresponds to a stabilizer ZX-diagram. We underline that throughout this work, all rewrites are valid *up to a scalar* since we are only concerned about making statements about com-

plexity. Keeping track of multiplicative scalar factors that arise under diagram rewriting can be done efficiently.

2 Simplifying Qubit ZX-Diagrams

Qubit ZX-diagrams are generated by *spiders*, whose *legs* or *wires* carry vector spaces of dimension $d = 2$. Diagrams are read bottom-to-top; bottom open wires (not connected to anything) are *input wires* and top ones are *outputs*. Diagrams with only outputs are called *states* and those with only inputs are called *effects*. A *closed* diagram is one with no inputs nor outputs and represents a *scalar*.

Spiders can be *composed*; placing diagrams side by side represents parallel composition ($\otimes$), with concrete interpretation the tensor product. Vertically stacking diagrams corresponds to sequential composition ($\circ$) and concretely means matrix multiplication. Specifically, it means tensor contraction along spider-legs; the common tensor indices represented by these wires are summed over. The concrete representation of these operations of course depends on the (semi)ring over which the spiders are interpreted as tensors. For spiders S and S' we write: $[\![S \otimes S']\!] = [\![S]\!] \otimes [\![S']\!]$, $[\![S \circ S']\!] = [\![S]\!] \cdot [\![S']\!]$.

Spiders come in two species: green Z-spiders and red X-spiders, decorated by a *phase* $\alpha \in [0, 2\pi)$. When $\alpha = 0$, we will omit it. The *standard representation* of the spider generators as tensors over $\mathbb{C}$ is:

$$\left[\!\!\left[\ \underset{n}{\underbrace{\overset{\overbrace{}^{m}}{\underset{\cdots}{\underset{\alpha}{\cdots}}}}}\ \right]\!\!\right] = |0\rangle^m \langle 0|^n + e^{i\alpha} |1\rangle^m \langle 1|^n\ , \quad \left[\!\!\left[\ \underset{n}{\underbrace{\overset{\overbrace{}^{m}}{\underset{\cdots}{\underset{\alpha}{\cdots}}}}}\ \right]\!\!\right] = |+\rangle^m \langle +|^n + e^{i\alpha} |-\rangle^m \langle -|^n$$

(1)

where $\{|0\rangle, |1\rangle\}$ is the *Z-basis* and $|\pm\rangle = |0\rangle \pm |1\rangle$ the *X-basis* in $\mathbb{C}^2$, in Dirac notation. The Hadamard gate H, whose function is to switch between the Z and X bases, is denoted as a yellow box. Often we will instead draw a dashed blue line to represent a *Hadamard edge*:

$$\ \ \square\ \ =\ \ \vdots\ \ =\ \ \overset{\frac{\pi}{2}}{\underset{\frac{\pi}{2}}{\frac{\pi}{2}}}\ \ ,\qquad \left[\!\!\left[\ \ \square\ \ \right]\!\!\right] \simeq |0\rangle \langle 0| + |0\rangle \langle 1| + |1\rangle \langle 0| - |1\rangle \langle 1| \quad (2)$$

The ZX-calculus is universal for multilinear maps; any tensor with entries in $\mathbb{C}$ has a corresponding ZX-diagram. The rewrite rules of the ZX-calculus (see Fig.1 in Appendix A) allow manipulation of the diagrams by *rewrites*. Importantly, up to a scalar, the rewrites are sound; they *preserve the semantics*, i.e. the concrete tensor representation over $\mathbb{C}$. The ZX-calculus is also *complete* in the sense that any true equation between tensors can be proven *only* in terms of rewrites. This gives ZX the status of a 'calculus'. What is important about qubit ZX-diagrams is that *only topology matters*; the concrete tensor semantics

of the diagram are invariant under deformations of the network as long as the inter-spider connectivity is respected.

The *stabilizer fragment* of the calculus consists of all diagrams in which all phases are $\alpha = \frac{\pi n}{2}$, $n \in \mathbb{Z}$. In (Theorem 5.4, [9]) the authors give an efficient algorithm for simplifying any qubit ZX-diagram to an equivalent diagram with fewer (see Appendix A.1). The algorithm consists of consecutive applications of *spider-eliminating rewrites*. In particular, this algorithm will *efficiently* simplify any closed stabilizer diagram until it contains at most one spider, at which point the scalar it represents can be easily read off. By 'efficiently' we mean via a sequence of spider elimination rewrites whose cost is polynomial in the initial number of spiders and their legs. Note each such rewrite updates only a polynomial number of edges in the diagram, which prevents an overwhelming memory cost of the simplification procedure.

3   Simplifying Qutrit ZX-Diagrams

We now turn to the qutrit ZX-calculus and examine the analogous story to that of the previous subsection, but now for the case where the dimension of the vector space carried by the wires is $d = 3$.

Qutrit spiders again come in two species, Z (green) and X (red), with the three-dimensional *Z-basis* $\{|0\rangle, |1\rangle, |2\rangle\}$. Let $\omega = e^{i\frac{2\pi}{3}}$ denote the third root of unity with $\bar{\omega} = \omega^2$ its complex conjugate. The qutrit *X-basis* is: $\{|+\rangle = \frac{1}{\sqrt{3}}(|0\rangle + |1\rangle + |2\rangle), |\omega\rangle = \frac{1}{\sqrt{3}}(|0\rangle + \omega|1\rangle + \bar{\omega}|2\rangle), |\bar{\omega}\rangle = \frac{1}{\sqrt{3}}(|0\rangle + \bar{\omega}|1\rangle + \omega|2\rangle)\}$. Spiders carry *two* phases α and β, and have the following *standard representation* as linear maps:

$$\left[\!\!\left[\overbrace{\underset{n}{\underbrace{\cdots}}}^{m}_{\substack{\alpha \\ \beta}} \right]\!\!\right] = |0\rangle^{\otimes m}\langle 0|^{\otimes n} + e^{i\alpha}|1\rangle^{\otimes m}\langle 1|^{\otimes n} + e^{i\beta}|2\rangle^{\otimes m}\langle 2|^{\otimes n} \tag{3}$$

$$\left[\!\!\left[\overbrace{\underset{n}{\underbrace{\cdots}}}^{m}_{\substack{\alpha \\ \beta}} \right]\!\!\right] = |+\rangle^{\otimes m}\langle +|^{\otimes n} + e^{i\alpha}|\omega\rangle^{\otimes m}\langle \omega|^{\otimes n} + e^{i\beta}|\bar{\omega}\rangle^{\otimes m}\langle \bar{\omega}|^{\otimes n} \tag{4}$$

When $\alpha = \beta = 0$ we will again omit the angles entirely, and just draw a small green or red dot. Throughout our work, whenever we use an integer n as a spider decoration, this is a shorthand for $\frac{2\pi}{3}n$. Since spider phases hold mod 2π, these integer decorations hold mod 3. Unless otherwise stated, we will use Greek letters to denote general angles, and Roman letters for these integer shorthands.

Hadamard gates are no longer self-adjoint, so we change our notation: we let a yellow box decorated with a 1 (mod 3) denote a Hadamard gate, while decorating with a 2 (mod 3) denotes its adjoint. We will shortly explain this choice. We also use a dashed blue line for the *Hadamard edge* (*H-edge*) and a purple dashed line for its adjoint (*$H^\dagger$-edge*). Those familar with the ZH-calculus should note that this notation is *not* analogous to the H-boxes therein.

$$
\boxed{1} \;=\; \Big\vert \;=\; \begin{smallmatrix}2\\2\\2\\2\\2\\2\end{smallmatrix} \;,\qquad\qquad \boxed{2} \;=\; \Big\vert \;=\; \begin{smallmatrix}1\\1\\1\\1\\1\\1\end{smallmatrix} \;,\qquad\qquad \boxed{0} \;=\; \begin{smallmatrix}\circ\\\circ\end{smallmatrix} \qquad (5)
$$

The last equation above says that in a graph-like diagram (which we will define shortly), a Hadamard edge decorated by a 0 is in fact not an edge at all, thanks to spider fusion. A very important difference from the qubit case is that in qutrit ZX-calculus there is no *plain* cap or cup:

$$
\smile \;\neq\; \smile \;,\qquad\qquad \frown \;\neq\; \frown \qquad (6)
$$

This has several consequences. Firstly, the maxim that *'only topology matters'* *no longer applies*. That is, it is now important to make clear the distinction between a spider's input and output wires, unlike in the qubit case where we could freely interchange the two. This gives the qutrit calculus a slightly more rigid flavour than its qubit counterpart. That said, this rigidity can be loosened; in particular, this distinction is irrelevant for H- and $H^\dagger$-edges [11]:

$$(7)$$

The set of rules of the qutrit ZX-calculus is shown in Figure 2 in Appendix A.

3.1   Graph-Like Qutrit ZX Diagrams

A *graph-like* qutrit ZX-diagram is one where every spider is green, spiders are only connected by blue Hadamard edges (*H-edges*) or their purple adjoints (*$H^\dagger$-edges*), every pair of spiders is connected by at most one H-edge or $H^\dagger$-edge, every input and output is connected to a spider, and every spider is connected to at most one input or output. A graph-like qutrit ZX-diagram is a *graph state* when every spider has zero phases and is connected to an output.

Note the difference compared to the qubit case: we need not worry about self-loops beacuse the qutrit ZX-calculus doesn't define a 'plain' cap or cup. But this comes at a cost: spiders in the qutrit case fuse more fussily. Specifically,

when two spiders of the same colour are connected by at least one plain edge and at least one H- or $H^\dagger$-edge, fusion is not possible. Instead, should we want to ensure we have a graph-like diagram, we can replace the plain wire:

$$
\tag{8}
$$

Indeed, we can show that every qutrit ZX-diagram is equivalent to a graph-like one. The following equations, derived in Appendix 1, are vital to this:

$$
\tag{9}
$$

This justifies our notation for Hadamard gates: we can think of Hadamard edges as 1-weighted edges and their adjoints as 2-weighted edges, then work modulo 3, since every triple of parallel edges disappears. Where the previous equations relate single H- and $H^\dagger$-boxes across multiple edges, the next three relate multiple H- and $H^\dagger$- boxes on single edges. They hold for $h \in \{1, 2\}$, and are proved via simple applications of rules (**id**), (**H**) and (**s**).

$$
\tag{10}
$$

Proposition 1. *Every qutrit ZX-diagram is equivalent to one that is graph-like.*

Proof. First use the colour change rule to turn all X-spiders into Z-spiders. Then use (10) to remove excess H- and $H^\dagger$-boxes, inserting a spider between any remaining consecutive pair of such boxes, so that all spiders are connected only by plain edges, H-edges or $H^\dagger$-edges. Fuse together as many as possible, and apply (8) where fusion is not possible, so that no plain edge connects two spiders. Apply (9) to all connected pairs of spiders until at most one H- or $H^\dagger$-edge remains between them. Finally, to ensure every input and output is connected to a spider and every spider is connected to at most one input or output, we can use (**H**) and (**id**) to add a few spiders, H- and $H^\dagger$-edges as needed:

$$
\tag{11}
$$

$$\square$$

A graph state is described fully by its underlying multigraph, or equivalently by an adjacency matrix, where edges take weights in $\mathbb{Z}_3$ (Lemma 4.2, [22]). Nodes correspond to phaseless green spiders, edges of weight 1 correspond to Hadamard edges, and edges of weight 2 correspond to $H^\dagger$-edges. As in the qubit case, graph states admit a *local complementation* operation (Definition 2.6, [22]), though the effect is now slightly more complicated. We'll give the intuition after the formal definition:

Definition 1. *Given $a \in \mathbb{Z}_3$ and a graph state G with adjacency matrix $W = (w_{i,j})$, the a-local complentation at node x is the new graph state $G *_a x$, whose adjacency matrix $W' = (w'_{i,j})$ is given by $w'_{i,j} = w_{i,j} + a w_{i,x} w_{j,x}$.*

So only those edges between neighbours of node x are affected. Specifically, for two nodes i and j both connected to x by the *same* colour edge, a-local complementation at x *increases* weight $w_{i,j}$ by a. If instead i and j are connected to x by edges of *different* colours, a-local complementation at x *decreases* $w_{i,j}$ by a. This is shown graphically below, and holds with the roles of blue and purple interchanged:

$$\tag{12}$$

Theorem 1. *(Theorem 4.4, Corollary 4.5, [22])   Given $a \in \mathbb{Z}_3$ and a graph state (G, W) containing a node x, let $N(x)$ denote the neighbours of x; that is, nodes i with weight $w_{i,x} \in \{1, 2\}$. Then the following equality holds:*

$$\tag{13}$$

Definition 2. *Given $a, b, c \in \mathbb{Z}_3$ and a graph state G containing nodes i and j, the (a, b, c)-pivot along ij is the new graph state $G \wedge_{(a,b,c)} ij := ((G *_a i) *_b j) *_c i$.*

This pivot operation again leads to an equality, up to introducing some extra gates on outputs, whose proof is found in Appendix 7. Here we shall only consider an $(a, -a, a)$-pivot along an edge ij of non-zero weight, for $a \in \{1, 2\}$. We will call this a *proper a-pivot* along ij, and denote it $G \wedge_a ij$.

Theorem 2. *Given $a \in \mathbb{Z}_3$ and a graph state (G, W) containing connected nodes i and j, define $N_=(i, j) := \{x \in N(i) \cap N(j) \mid w_{x,i} = w_{x,j}\}$ and $N_{\neq}(i, j) := \{x \in N(i) \cap N(j) \mid w_{x,i} \neq w_{x,j}\}$. Then the following equation relates G and its*

proper a-pivot along ij:

$$\tag{14}$$

3.2   Qutrit Elimination Theorems

We classify spiders into three families exactly as in (Theorem 3.1, [22]):


$$\tag{15}$$

We call a spider in a graph-like ZX-diagram *interior* if it isn't connected to an input or output. Given any graph-like ZX-diagram, we will show that we can eliminate standalone interior $\mathcal{P}$- and $\mathcal{N}$-spiders by local complementation, and pairs of connected interior $\mathcal{M}$-spiders by pivoting.

First, we define a modification of the *!-box* notation, as introduced in [8] for general string diagrams. A !-box is a compressed notation for a *family* of diagrams; the contents of the !-box are 'repeated' or 'unfolded' $n \geq 0$ times. Following the style of [3], we allow a parameter denoting the maximum number of copies. We also extend this notation as follows: we decorate the !-box with an edge-type, which denotes that the spiders unfolded are all-to-all connected by an edge of this type. In qutrit ZX-diagrams this notation is well-defined in certain scenarios: in particular, when the denoted edge-type is a H- or $H^\dagger$-edge (since then the distinction between a spider's input and output wires disappears) and the main contents of the !-box is equivalent to a single spider (since then there is no ambiguity about which spiders are connected). For example:
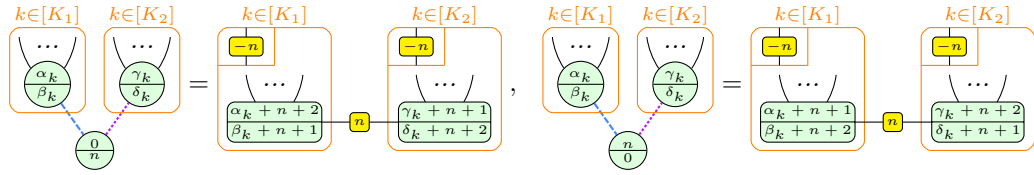

Theorem 3. *Given any graph-like ZX-diagram containing an interior $\mathcal{P}$-spider x with phase $\boxed{\frac{p}{p}}$ for $p \in \{1, 2\}$, suppose we perform a p-local complementation*

*at x. Then the new ZX-diagram is related to the old one by the following equality:*
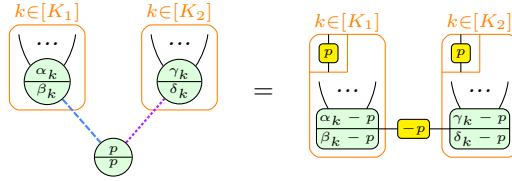
Theorem 4. *Given any graph-like ZX-diagram containing an interior $\mathcal{N}$-spider x with phase $\boxed{\frac{0}{n}}$ or $\boxed{\frac{n}{0}}$ for $n \in \{1, 2\}$, suppose we perform a $(-n)$-local complementation at x. Then, treating the two cases separately, the new ZX-diagrams are related to the old ones by the equalities:*

Theorem 5. *Given any graph-like ZX-diagram containing two interior $\mathcal{M}$-spiders i and j connected by edge ij of weight $w_{i,j} =: w \in \{1, 2\}$, suppose we perform a proper $\pm w$-pivot along ij (both choices give the same result). For $w = 1$, the new ZX-diagram is related to the old one by the following equality:*
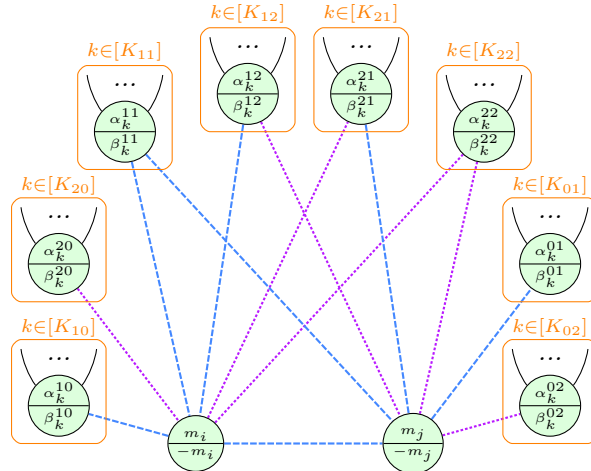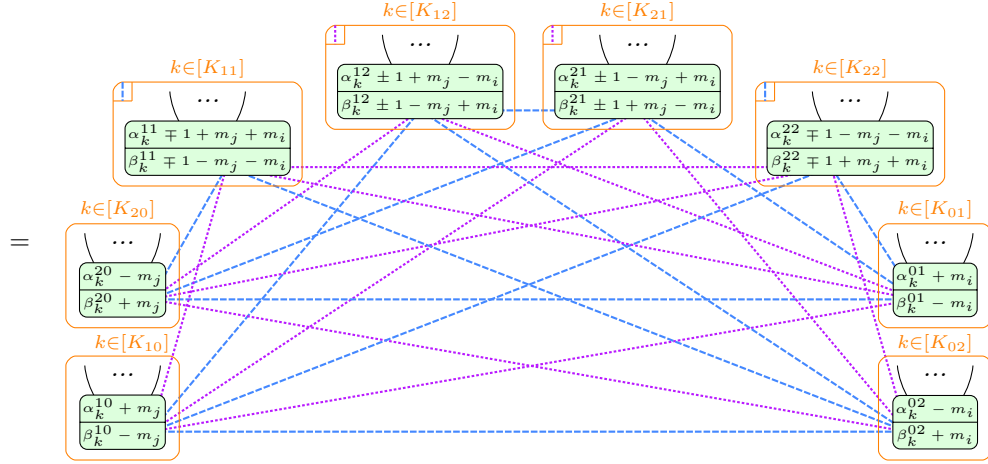
The case $w = 2$ differs only as follows: in the first diagram (the left hand side of the equation), the edge ij is purple (by definition), while in the lower diagram (the right hand side of the equation), a $\pm 2 = \mp 1$ will replace all occurences of ± 1, and the roles of purple and blue will be swapped throughout.

Proofs of these theorems are found in Appendix 8, 9 and 10 respectively. We can now combine them into an algorithm for efficiently simplifying a *closed* graph-like ZX-diagram. First note that after applying any one of the three elimination theorems to such a diagram, and perhaps removing parallel H- or $H^\dagger$-edges via (9), we again have a graph-like diagram.

Theorem 6. *Given any closed graph-like ZX-diagram, the following algorithm will always terminate after a finite number of steps, returning an equivalent graph-like ZX-diagram with no $\mathcal{N}$-spiders, $\mathcal{P}$-spiders, or adjacent pairs of $\mathcal{M}$-spiders. Repeat the steps below until no rule matches. After each step, apply (9) as needed until the resulting diagram is graph-like:*

1. *Eliminate a $\mathcal{P}$-spider via Theorem 3.*
2. *Eliminate an $\mathcal{N}$-spider via Theorem 4.*
3. *Eliminate two adjacent $\mathcal{M}$-spiders via Theorem 5.*

Proof. At every step the total number of spiders decreases by at least one, so since we start with a finite diagram the algorithm terminates after a finite number of steps. By construction, when it does so we are left with an equivalent graph-like ZX-diagram with no $\mathcal{N}$-spiders, $\mathcal{P}$-spiders, or adjacent pairs of $\mathcal{M}$-spiders. $\square$

In particular, if we start with a stabilizer diagram, we can eliminate all but perhaps one spider, depending on whether the initial number of $\mathcal{M}$-spiders was odd or even. This is because no step introduces any non-stabilizer phases. The algorithm above could be extended to a *non-closed* graph-like diagrams as in (Theorem 5.4, [9]) as part of a qutrit circuit optimisation algorithm, by supplementing with a method for circuit extraction method. We leave this for future work.

4   Case studies

In this section we present two problems which can naturally be cast in tensor network form. These problem families are interesting in that they show a transition in complexity from easy to hard when the dimension d carried by the wires is greater than a specific value. We recast known results about evaluating the *Jones polynomial*, and finally we briefly look at graph colouring.

4.1   Jones Polynomial at Lattice Roots of Unity

A *knot K* is a circle embedded in $\mathbb{R}^3$. A set of knots tangled together make a *link L*. A link L can be represented by a *link diagram* by projecting it on to the plane but retaining the information of over or under crossings. We say that $L \simeq L'$ iff the diagram of link L can be deformed to that of link L' without cutting or gluing strands, or passing strands through each other. The Jones polynomial $V_L(t)$ is a Laurent polynomial in a variable $t \in \mathbb{C}$ and is a *link invariant*. This means that $V_L(t) \neq V_{L'}(t) \Rightarrow L \not\simeq L'$.

In general, computing $V_L(t)$ is exponentially costly in the number of crossings c, something made explicit when one uses the Kauffman bracket method [15]. Exactly evaluating the Jones polynomial at points $t \in \mathbb{C}$ is #P-hard, *except* at the *lattice roots of unity* $\Lambda = \{\pm 1, \pm i, \pm e^{i2\pi/3}, \pm e^{i4\pi/3}\}$, where it can be evaluated at cost $O(poly(c))$ [14].

Additively approximating the Jones polynomial at *non-lattice roots of unity* is a paradigmatic BQP-complete complete problem [2,16]. Topological quantum computation [10,19] is the most natural model for such knot theoretic questions. In this model, quantum states are defined in the fusion space of *anyons*, emergent quasiparticles with nontrivial exchange statistics arising in two-dimensional exotic phases of matter. Quantum computation is performed by creating anyons from the vacuum, then braiding them, and finally fusing them back to the vacuum, where braids play the role of unitary gates. The world-lines of the anyons define a closed braid, i.e. a link. Such a link encodes a quantum amplitude corresponding to its Jones polynomial evaluated at a root of unity depending on the anyon theory at hand [25]. Specifically, in the case of $\mathrm{SU}(2)_k$ anyons, the Jones polynomial is evaluated at $t(k) = e^{i2\pi/(2+k)}$ [20].

Also, the evaluation of the Jones polynomial at certain points can be expressed, up to an efficiently computable scalar that depends on the link diagram, as the partition function $Z_{G_L}(d)$ of a d-state Potts model with suitable spin-spin interactions [26]. This Potts model is defined on a signed graph G_L, obtained as follows. The link diagram is bicoloured checkerboard-style, then every coloured area is mapped to a vertex and every crossing is mapped to a signed edge according its orientation relative to the surrounding colours, as in (16) below. The relation between the point $t(d)$ at which the Jones polynomial is evaluated and the dimension d of the spins is $d = t + t^{-1} + 2$, which can be solved for $t(d)$ [18].

Note the correspondence between the dimension d in the Potts approach and the level k in the anyon-braiding approach to the Jones polynomial: $\{t(d)|\ d \in \{1,2,3,4\}\} = \{t(k)|\ k \in \{1,2,4,\infty\}\} \subseteq \Lambda$. This is consistent with the fact that

braiding $SU(2)_2$ anyons (Ising) or $SU(2)_4$ anyons is not universal (unless the $SU(2)_4$ anyons are augmented by fusion and measurements [17]).

The partition function $Z_{G_L}(d \in \mathbb{N})$ can be expressed as a closed tensor network in terms of phaseless (green) d-dimensional Z-spiders connected via wires that go through $\pm$-*boxes* [18]:

$$(16)$$

The $\pm$-boxes have the following concrete interpretation as matrices:

$$
\left[\!\!\left[\pm \right]\!\!\right] = \sum_{i,j=0}^{d-1} (1-(1+t(d)^{\mp 1})\delta_{ij})\,|i\rangle\langle j| = \begin{pmatrix} -t(d)^{\mp 1} & 1 & \dots & 1 \\ 1 & -t(d)^{\mp 1} & \dots & 1 \\ \vdots & \vdots & \ddots & \vdots \\ 1 & 1 & \dots & -t(d)^{\mp 1} \end{pmatrix}
$$

$$(17)$$

The $\pm$-matrices above for $d \in \{2,4\}$ are equal up to a scalar to concrete interpretations of *qubit stabilizer* ZX-diagrams, and the $\pm$-matrices for $d = 3$ of *qutrit stabilizer* ZX-diagrams (see Appendix 3):

$$
\left[\!\!\left[\pm \right]\!\!\right]_{d=2} \simeq \left[\!\!\left[\pm \tfrac{\pi}{2} \right]\!\!\right] , \quad \left[\!\!\left[\pm \right]\!\!\right]_{d=3} \simeq \left[\!\!\left[\substack{\pm 1 \\ \pm 1} \right]\!\!\right] , \quad \left[\!\!\left[\pm \right]\!\!\right]_{d=4} \simeq \left[\!\!\left[\pi - \pi \right]\!\!\right]
$$

$$(18)$$

Since these generators decompose as stabilizer diagrams, $Z_{G_L}(d \in \{2,3,4\})$ can be evaluated *efficiently* via stabilizer ZX-diagram simplification. Thus, we recover the known result that evaluating the Jones polynomial at $t \in \Lambda$ is in P. On the other hand, computing $Z_{G_L}(d \geq 5)$ is #P-hard.

4.2   Graph Colouring

Finally, let us briefly look at the *graph colouring problem*, or evaluating the chromatic polynomial. A *d-colouring* of a graph G is an assignment of colours $\{1,...,d\}$ to the vertices of G so that no neighbouring vertices have the same colour. Given a graph G and an integer d, we wish to *count* the number of such d-colourings. Again, this problem can be interpreted as the zero-temperature partition function of an antiferromagnetic d-state Potts model [21]. Through the lens of our graphical exposition we see that counting problems and computing partition functions are essentially the same problem, since both can be straightforwardly encoded as closed tensor networks.

Given a graph G, the graph colouring problem can be encoded as a ZX-diagram as follows. Every vertex of the graph is mapped to a d-dimensional

phaseless (green) Z-spider which copies spin states so that they can enter into the X-boxes, each of which in turn enforces that spin states entering it are not the same.

$$(19)$$
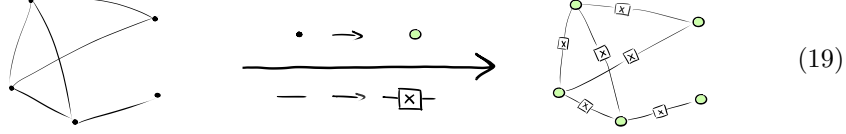
The X-boxes have the following concrete interpretation (as special case of the $\pm$-boxes, where $t = 0$), and for $d = 2$ they are just the Pauli X:

$$\left[\!\!\left[\; \boxed{X} \;\right]\!\!\right] \;=\; \sum_{i,j=0}^{d-1} (1-\delta_{ij})\,|i\rangle\langle j| \;=\; \begin{pmatrix} 0 & 1 & \dots & 1 \\ 1 & 0 & \dots & 1 \\ \vdots & \vdots & \ddots & \vdots \\ 1 & 1 & \dots & 0 \end{pmatrix} \;,\quad \left[\!\!\left[\; \boxed{X} \;\right]\!\!\right]_{d=2} \;\simeq\; \left[\!\!\left[\; \boxed{\pm\pi} \;\right]\!\!\right]$$

$$(20)$$

Counting k-colourings for $k \geq 3$ is a canonical #P-complete problem. For $k = 0, 1, 2$ the problem is in P [14]. For $k = 2$ this is witnessed by the fact that the problem reduces to simplifying a qubit stabilizer diagram, which can be done efficiently. However, for $d = 3$ the X-matrix cannot be expressed as a stabilizer qutrit diagram; we prove this using our qutrit elimination theorems in Appendix 4. This is consistent with the fact that counting 3-colourings is #P-complete.

5   Outlook

In this work, we fleshed out non-trivial simplifications strategies for qutrit ZX diagrams and we have advocated for the use of the ZX-calculus as a unifying graphical framework for treating a broad range of many-body problems on equal footing, and for diagnosing the complexity of interesting families of problems.

A main path for future work entails the generalisation of our stabilizer simplification rules to qudits of prime dimensions. This in turn also motivates work in circuit extraction [4] for qudit circuits; one could hope to find graph-theoretic simplification [9] strategies analogous to those for the case of qubits. Another direction regards defining scalar-exact versions of the rewrite rules, which would be necessary for concrete applications to problems where d-state systems are the native degrees of freedom.

6   Acknowledgments

14   Alex Townsend-Teague [1] and Konstantinos Meichanetzidis [1,2]

References

1. Aaronson, S., Gottesman, D.: Improved simulation of stabilizer circuits. Physical Review A **70**(5) (Nov 2004). https://doi.org/10.1103/physreva.70.052328, `http://dx.doi.org/10.1103/PhysRevA.70.052328`
2. Aharonov, D., Jones, V., Landau, Z.: A polynomial quantum algorithm for approximating the jones polynomial. Algorithmica **55**(3), 395â€"421 (Mar 2008). https://doi.org/10.1007/s00453-008-9168-0, `http://dx.doi.org/10.1007/s00453-008-9168-0`
3. Backens, M., Kissinger, A.: Zh: A complete graphical calculus for quantum computations involving classical non-linearity (2018)
4. Backens, M., Miller-Bakewell, H., de Felice, G., Lobski, L., van de Wetering, J.: There and back again: A circuit extraction tale (2020)
5. de Beaudrap, N., Kissinger, A., Meichanetzidis, K.: Tensor network rewriting strategies for satisfiability and counting (2020)
6. Coecke, B., Duncan, R.: Interacting quantum observables: categorical algebra and diagrammatics. New Journal of Physics **13**(4), 043016 (Apr 2011). https://doi.org/10.1088/1367-2630/13/4/043016, `http://dx.doi.org/10.1088/1367-2630/13/4/043016`
7. Damm, C., Holzer, M., McKenzie, P.: The complexity of tensor calculus. computational complexity **11**(1), 54–89 (2002). https://doi.org/10.1007/s00037-000-0170-4, `https://doi.org/10.1007/s00037-000-0170-4`
8. Dixon, L., Duncan, R.: Graphical reasoning in compact closed categories for quantum computation. Annals of Mathematics and Artificial Intelligence **56**(1), 23–42 (2009)
9. Duncan, R., Kissinger, A., Perdrix, S., van de Wetering, J.: Graph-theoretic simplification of quantum circuits with the zx-calculus (2020)
10. Freedman, M.H., Kitaev, A., Larsen, M.J., Wang, Z.: Topological quantum computation. Bulletin of the American Mathematical Society **40**(01), 31–39 (Oct 2002). https://doi.org/10.1090/s0273-0979-02-00964-3, `https://doi.org/10.1090/s0273-0979-02-00964-3`
11. Gong, X., Wang, Q.: Equivalence of local complementation and euler decomposition in the qutrit zx-calculus (2017)
12. Gong, X., Wang, Q.: Equivalence of local complementation and euler decomposition in the qutrit zx-calculus. arXiv preprint arXiv:1704.05955 (2017)
13. Gray, J., Kourtis, S.: Hyper-optimized tensor network contraction (2020)
14. Jaeger, F., Vertigan, D.L., Welsh, D.J.A.: On the computational complexity of the jones and tutte polynomials. Mathematical Proceedings of the Cambridge Philosophical Society **108**(1), 35â€"53 (1990). https://doi.org/10.1017/S0305004100068936
15. Kauffman, L.H.: Knots and Physics. WORLD SCIENTIFIC (Jul 2001). https://doi.org/10.1142/4256, `https://doi.org/10.1142/4256`
16. Kuperberg, G.: How hard is it to approximate the jones polynomial? (2014)
17. Levaillant, C., Bauer, B., Freedman, M., Wang, Z., Bonderson, P.: Universal gates via fusion and measurement operations onsu(2)4anyons. Physical Review A **92**(1) (Jul 2015). https://doi.org/10.1103/physreva.92.012301, `http://dx.doi.org/10.1103/PhysRevA.92.012301`
18. Meichanetzidis, K., Kourtis, S.: Evaluating the jones polynomial with tensor networks. Phys. Rev. E **100**, 033303 (Sep 2019). https://doi.org/10.1103/PhysRevE.100.033303, `https://link.aps.org/doi/10.1103/PhysRevE.100.033303`

19. Pachos, J.K.: Introduction to Topological Quantum Computation. Cambridge University Press (2012). https://doi.org/10.1017/CBO9780511792908
20. Rowell, E.C., Wang, Z.: Mathematics of topological quantum computing. Bulletin of the American Mathematical Society **55**(2), 183â€"238 (Jan 2018). https://doi.org/10.1090/bull/1605, `http://dx.doi.org/10.1090/BULL/1605`
21. Sokal, A.D.: Chromatic polynomials, potts models and all that (1999). https://doi.org/10.1016/S0378-4371(99)00519-1
22. Wang, Q.: Qutrit zx-calculus is complete for stabilizer quantum mechanics (2018)
23. Wang, Q.: Completeness of algebraic zx-calculus over arbitrary commutative rings and semirings (2020)
24. van de Wetering, J.: Zx-calculus for the working quantum computer scientist (2020)
25. Witten, E.: Quantum field theory and the jones polynomial. Communications in Mathematical Physics **121**(3), 351–399 (Sep 1989). https://doi.org/10.1007/bf01217730, `https://doi.org/10.1007/bf01217730`
26. Wu, F.Y.: Knot theory and statistical mechanics. Rev. Mod. Phys. **64**, 1099–1131 (Oct 1992). https://doi.org/10.1103/RevModPhys.64.1099, `https://link.aps.org/doi/10.1103/RevModPhys.64.1099`

A   Qubit ZX Calculus

The well-known rewrite rules of the qubit ZX-calculus are shown in Fig.1.

A.1   Stabilizer Qubit ZX Diagrams

The *stabilizer fragment* of the calculus consists of all diagrams in which all phases are $\alpha = \frac{\pi n}{2}$, $n \in \mathbb{Z}$. In (Theorem 5.4, [9]) the authors give an efficient algorithm for simplifying any qubit ZX-diagram to an equivalent diagram with fewer spiders. The algorithm consists of consecutive applications of spider-eliminating rewrites.

Every diagram is equivalent to a *graph-like* diagram: every spider is green, every edge is a Hadamard edge, there are no parallel edges or self-loops, every input and output wire is connected to a spider and every spider has at most one input or output wire. The following derivable rules are key to this:

$$(21)$$

Then the following two rewrite rules, derived via *local complementation* and *pivoting*, can be used to eliminate spiders:

$$(22)$$
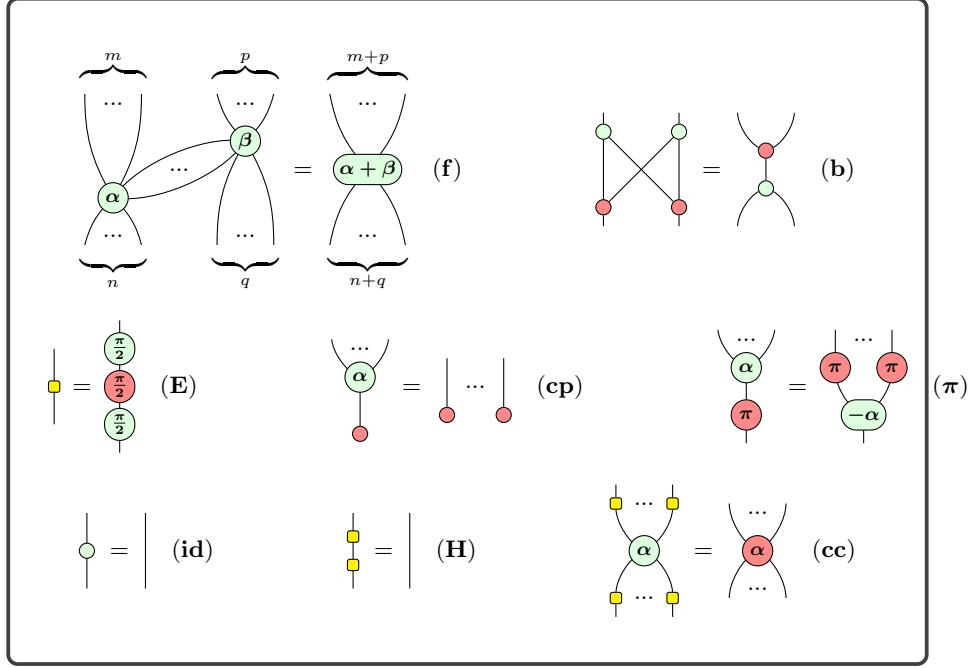
Fig. 1: Rewrite rules for the qubit ZX-calculus where spiders are interpreted as tensors over $\mathbb{C}$.

$$(23)$$

For more details, see (Section 4, [9]). Eq. (22) says that we can remove any spider with phase $\pm\frac{\pi}{2}$ at the cost of performing a local complementation at said spider. Furthermore, Eq. (23) says we can remove any pair of spiders with phases in $\{0, \pi\}$ connected by a Hadamard edge at the cost of performing a pivot along said edge. After each application of (22) or (23), we can use (21) to remove any parallel Hadamard edges and ensure the diagram remains graph-like.

B   Qutrit ZX Calculus

We now give a full set of rules defining the qutrit ZX-calculus. Our presentation aims for clarity and accessibility; for a more rigourous description, see [22].
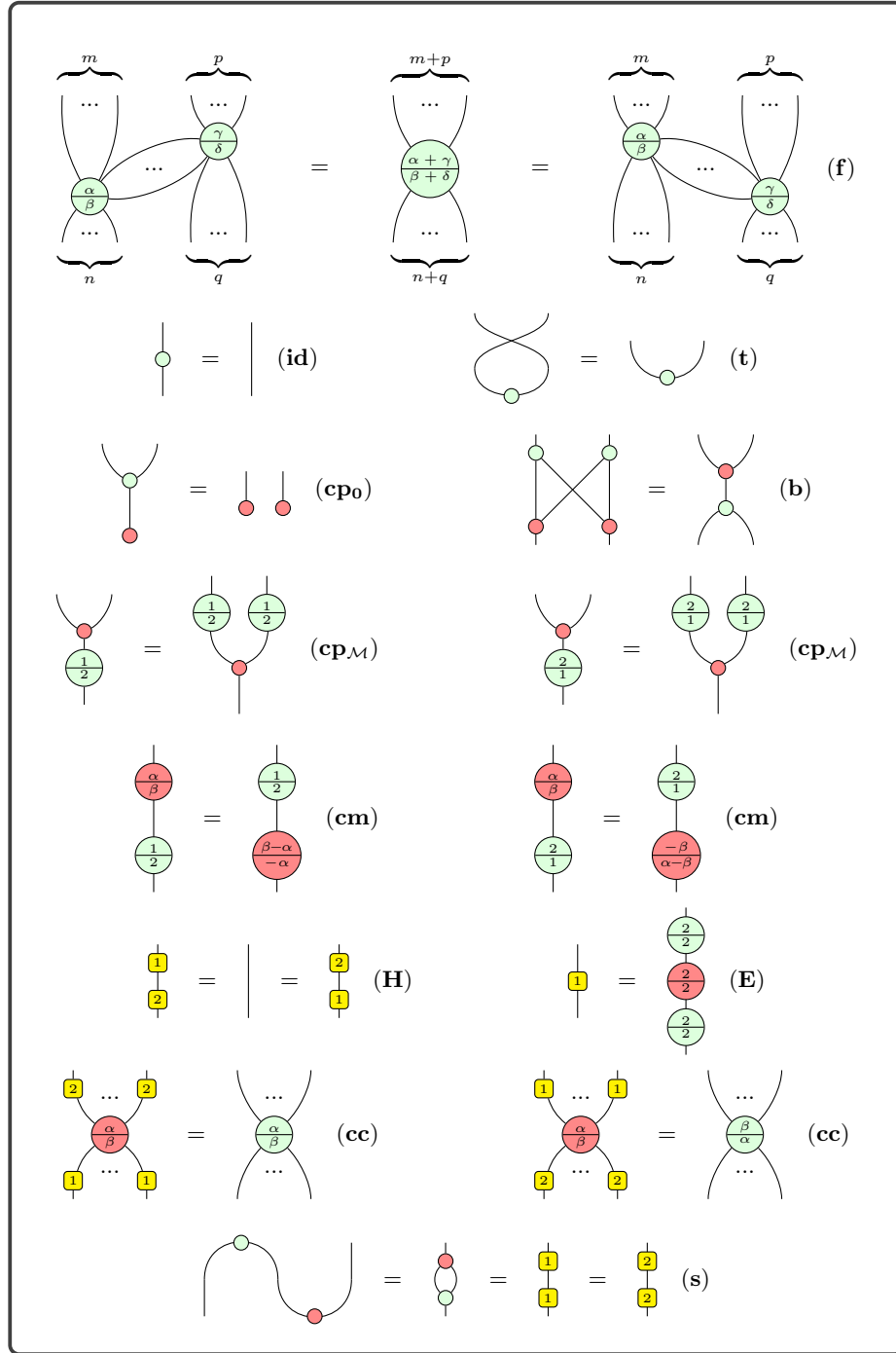
Fig. 2: Rewrite rules for the qutrit ZX-calculus where spiders are interpreted as tensors over $\mathbb{C}$.

Definition 3. *The qutrit ZX-calculus is a graphical calculus generated by the following diagrams, where $\alpha, \beta \in [0, 2\pi]$:*

$$\left\{ \quad , \quad , \quad , \quad , \quad \right\} \tag{24}$$

and their adjoints $(-)^\dagger$. Adjoints are found by swapping inputs and outputs and negating any decorations - recall negation is mod 2π for general spider phases, and mod 3 for integer spider phases and Hadamard boxes. Thus the two rightmost generators are self-adjoint, whereas the first three satisfy:

$$\left(\right)^\dagger = \quad , \qquad \left(\right)^\dagger = \quad , \qquad \left(\right)^\dagger = \tag{25}$$

These generators can be composed in parallel ($\otimes$) and sequentially ($\circ$), and the resulting diagrams are governed by the rewrite rules in Figure 2, wherein addition is modulo 2π. The fusion rule ($\mathbf{f}$) applies to spiders of the same colour connected by at least one wire. Importantly, all the rules hold under taking adjoints, where for diagrams D and E we have:

$$(D \otimes E)^\dagger = D^\dagger \otimes E^\dagger \;, \qquad\qquad (D \circ E)^\dagger = D^\dagger \circ E^\dagger \tag{26}$$

Furthermore, it can be derived that all but the commutation equations ($\mathbf{cm}$) and the colour change equations ($\mathbf{cc}$) continue to hold when the roles of green and red (i.e. Z and X) are interchanged. For these four exceptions, however, analogous equations can be derived from the existing ones; for example, the corresponding colour change equations will be relevant for us later.

Proposition 2. *The following equations are derivable in the qutrit ZX-calculus:*

$$= \quad , \qquad = \tag{27}$$

Proof. Add H- and $H^\dagger$-boxes to both sides of the original colour change equations in such a way that we can then cancel Hadamards on the legs of the red spiders via ($\mathbf{H}$). $\qquad\qquad\square$

Lemma 1. *The following equations hold in the qutrit ZX-calculus:*

$$(28)$$

Proof. It is shown in Lemma 2.8 [11] that the qutrit ZX-calculus satisfies the following 'Hopf law':

$$(29)$$

Therefore, to prove the first equation, we can argue as follows, for $h \in \{1, 2\}$:

$$(30)$$

The other two equations are proved in (Lemma 3.4, [12]). □

C   Pivoting in the Qutrit ZX-Calculus

Next we prove the pivot equality from Theorem 2. We require the following: since (**E**) holds under taking adjoints, and swapping the roles of red and green, we have:


$$(31)$$

Theorem 7. / *Theorem 2.* *Given $a \in \mathbb{Z}_3$ and a graph state (G, W) containing connected nodes i and j, define $N_=(i, j) := \{x \in N(i) \cap N(j) \mid w_{x,i} = w_{x,j}\}$ and $N_{\neq}(i, j) := \{x \in N(i) \cap N(j) \mid w_{x,i} \neq w_{x,j}\}$. Then the following equation relates*

G and its proper a-pivot along ij:

$$\tag{32}$$

Proof. There are four cases $(a, w_{i,j} \in \{1, 2\})$, which split into two pairs of symmetric cases: $a = w_{i,j}$ and $a \neq w_{i,j}$. We show just one case - the 1-pivot along ij of weight 1 - the remaining cases being analogous. We again employ the !-notation. An asterisk $*_a$ next to a spider means that at the next step an a-local complementation will be performed at this spider.

$$\overset{1}{=}$$

$$\overset{(\mathbf{f})}{\underset{=}{(31)}}$$
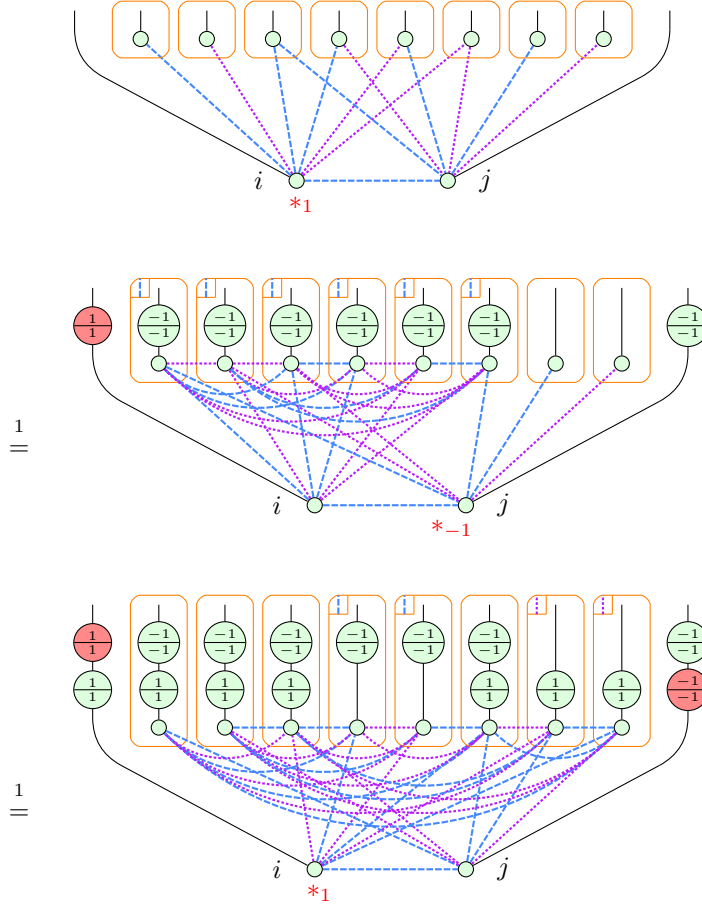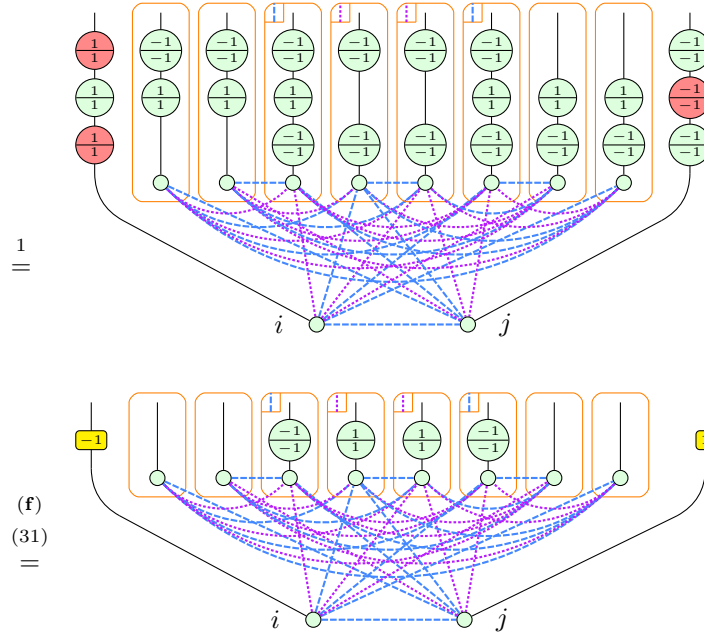
D Spider Elimination Rules for Qutrit ZX

Now we prove the three elimination theorems for $\mathcal{P}$-, $\mathcal{N}$- and $\mathcal{M}$-spiders. All three require the following two lemmas.

Lemma 2. *The following 'leg flip' equation holds in the qutrit ZX-calculus:*

$$\tag{33}$$

Proof.

$$\tag{34}$$

Lemma 3. *The following more substantial 'M-copy' rule holds in the qutrit ZX-calculus, for any M-spider state (i.e. $m \in \{0, 1, 2\}$ below):*

$$(35)$$

Proof. First we prove that an $\mathcal{M}$-spider with non-trivial phase (i.e. $m \in \{1, 2\}$) satisfies a copy rule exactly like the rule $(\mathbf{cp_0})$:

$$(36)$$

Then we prove the case $\alpha = \beta = 0$ by induction:

$$(37)$$

Which finally allows us to prove the full statement, where the last equality is just dropping the scalar term:

$$(38)$$

$\square$

D.1 $\mathcal{P}$-spider Elimination

The $\mathcal{P}$-spider elimination theorem additionally requires a lemma allowing us to turn a $\mathcal{P}$-spider state of one colour into a $\mathcal{P}$-spider state of the other. We will use this lemma its adjoint form in the proof of the main theorem.

Lemma 4. *The following rule holds in the qutrit ZX-calculus, for $p \in \{1, 2\}$:*

$$(39)$$

Proof.

$$
\begin{array}{ccccccccc}
\vcenter{\hbox{\includegraphics{}}} & \overset{(\mathbf{cc})}{=} & \vcenter{\hbox{\includegraphics{}}} & \overset{(31)}{=} & \vcenter{\hbox{\includegraphics{}}} & \overset{(\mathbf{f})}{=} & \vcenter{\hbox{\includegraphics{}}} & \overset{3}{=} & \vcenter{\hbox{\includegraphics{}}} & \overset{(\mathbf{f})}{=} & \vcenter{\hbox{\includegraphics{}}}
\end{array}
\tag{40}
$$

$\square$

Theorem 8. / *Theorem 3.* *Given any graph-like ZX-diagram containing an interior $\mathcal{P}$-spider x with phase $\boxed{\substack{p\\p}}$ for $p \in \{1, 2\}$, suppose we perform a p-local complementation at x. Then the new ZX-diagram is related to the old one by the following equality:*

$$
\vcenter{\hbox{\includegraphics{}}}
\;=\;
\vcenter{\hbox{\includegraphics{}}}
$$

Proof. For clarity of presentation we only show the case $\boxed{\substack{p\\p}} = \boxed{\substack{1\\1}}$, the other case being near-identical.

$$
\vcenter{\hbox{\includegraphics{}}}
\;\overset{(\mathbf{f})}{=}\;
\vcenter{\hbox{\includegraphics{}}}
\;\overset{1}{=}\;
\vcenter{\hbox{\includegraphics{}}}
$$

$$
\overset{(\mathbf{f})}{\underset{4}{=}}
\vcenter{\hbox{\includegraphics{}}}
\;\overset{2}{=}\;
\vcenter{\hbox{\includegraphics{}}}
\;\overset{3}{=}\;
\vcenter{\hbox{\includegraphics{}}}
$$

$$(5) \atop = \qquad (\mathbf{cc}) \atop = \qquad (\mathbf{f}) \atop =$$

D.2 $\mathcal{N}$-spider Elimination

Proving the corresponding $\mathcal{N}$-spider elimination theorem again requires a lemma allowing us to turn an $\mathcal{N}$-spider state of one colour into an $\mathcal{N}$-spider state of the other.

Lemma 5. *The following rules hold in the qutrit ZX-calculus:*

$$\begin{array}{ccc} & & \\ \boxed{\tfrac{0}{1}} = \boxed{\tfrac{2}{0}} \,, & \boxed{\tfrac{0}{2}} = \boxed{\tfrac{0}{1}} \,, & \boxed{\tfrac{1}{0}} = \boxed{\tfrac{0}{2}} \,, & \boxed{\tfrac{2}{0}} = \boxed{\tfrac{1}{0}} \end{array} \qquad (41)$$

Proof. For any green $\mathcal{N}$-spider state with phase $\left(\tfrac{n}{n'}\right)$, we have a choice of two colour change rules which we could use to turn it into a red $\mathcal{N}$-spider state with a H- or $H^\dagger$-box on top:

$$\underset{\tfrac{n}{n'}}{\boxed{2}} \overset{(\mathbf{cc})}{=} \left(\tfrac{n}{n'}\right) \overset{(\mathbf{cc})}{=} \underset{\tfrac{n'}{n}}{\boxed{1}} \qquad (42)$$

Of these two choices, exactly one has a decomposition of of the H-/$H^\dagger$-box as in (31) that allows the bottom two red spiders to fuse into an $\mathcal{M}$-spider, which we can then move past the green spider above it via 3. For brevity we only show the case $\left(\tfrac{n}{n'}\right) = \left(\tfrac{0}{1}\right)$:

$$\left(\tfrac{0}{1}\right) \overset{(\mathbf{cc})}{=} \underset{\tfrac{0}{1}}{\boxed{2}} \overset{(31)}{=} \begin{smallmatrix} \tfrac{1}{1} \\ \tfrac{1}{1} \\ \tfrac{1}{1} \\ \tfrac{0}{1} \end{smallmatrix} \overset{(\mathbf{f})}{=} \begin{smallmatrix} \tfrac{1}{1} \\ \tfrac{1}{1} \\ \tfrac{1}{2} \end{smallmatrix} \overset{3}{=} \begin{smallmatrix} \tfrac{1}{1} \\ \tfrac{1}{2} \end{smallmatrix} \overset{(\mathbf{f})}{=} \left(\tfrac{2}{0}\right) \qquad (43)$$

Corollary 1. *The following equations hold in the qutrit ZX-calculus, for $n \in \{1,2\}$:*

$$\begin{array}{cc} \left(\tfrac{0}{n}\right) & \left(\tfrac{n}{0}\right) \\ \underset{\tfrac{-n}{-n}}{\bigcirc} = \left(\tfrac{2}{1}\right) \,, & \underset{\tfrac{-n}{-n}}{\bigcirc} = \left(\tfrac{1}{2}\right) \end{array} \qquad (44)$$

Proof. Again we only prove one case, the other three being analogous. Each case uses 5 in its adjoint form - recall that the adjoint of a spider is found by swapping inputs and outputs and negating angles.
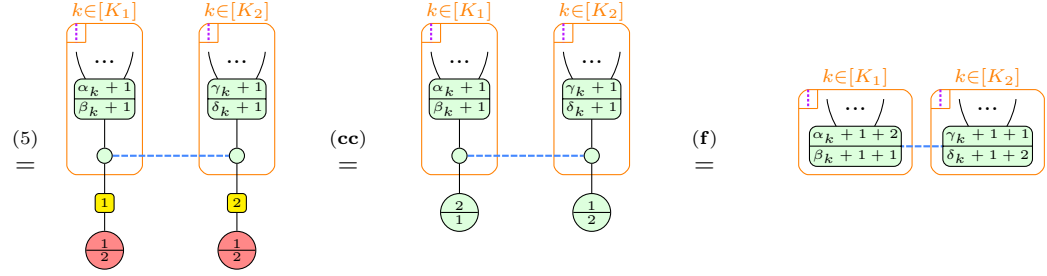

$$(45)$$

$\square$

Theorem 9. / *Theorem 4.* *Given any graph-like ZX-diagram containing an interior $\mathcal{N}$-spider x with phase $\boxed{\frac{0}{n}}$ or $\boxed{\frac{n}{0}}$ for $n \in \{1, 2\}$, suppose we perform a $(-n)$-local complementation at x. Then, treating the two cases separately, the new ZX-diagrams are related to the old ones by the equalities:*

Proof. We prove the case where x has phase $\boxed{\frac{0}{1}}$, the other cases being near-identical.

D.3 $\mathcal{M}$-spider Elimination

Theorem 10. / *Theorem 5.* *Given any graph-like ZX-diagram containing two interior $\mathcal{M}$-spiders i and j connected by edge ij of weight $w_{i,j} =: w \in \{1, 2\}$, suppose we perform a proper $\pm w$-pivot along ij (both choices give the same result). For $w = 1$, the new ZX-diagram is related to the old one by the following equality:*

$=$

$k \in [K_{11}]$

$\alpha_k^{11} \mp 1 + m_j + m_i$
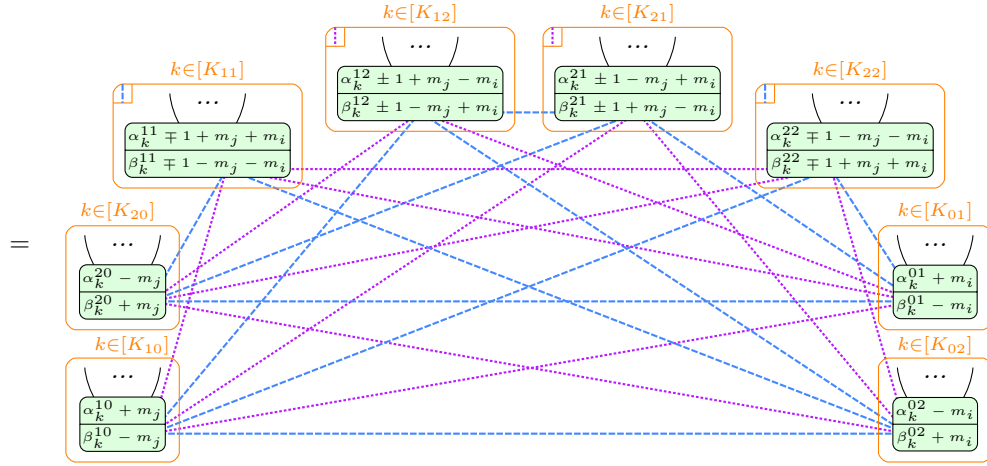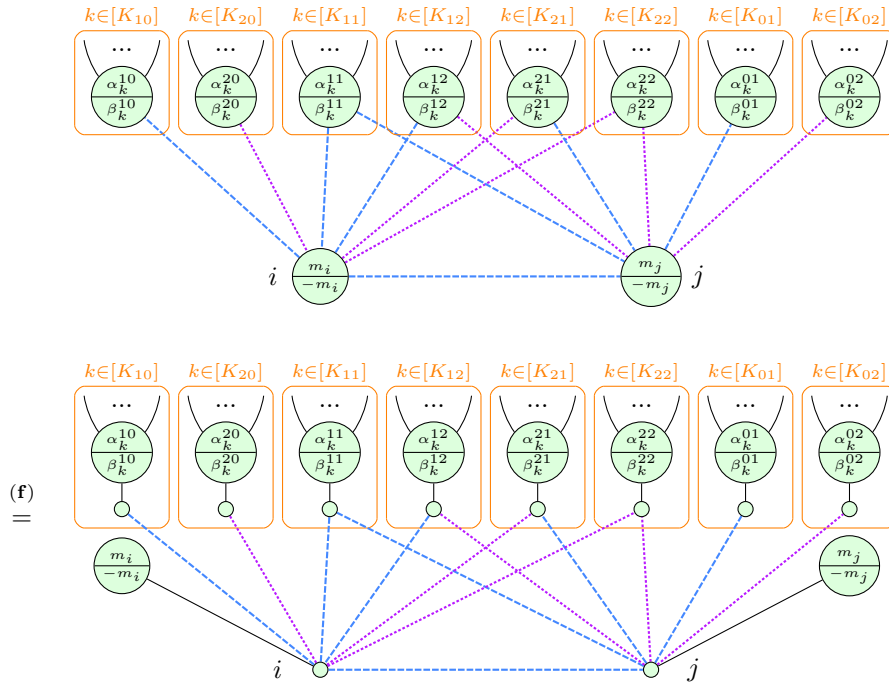$\beta_k^{11} \mp 1 - m_j - m_i$

$k \in [K_{12}]$

$\alpha_k^{12} \pm 1 + m_j - m_i$
$\beta_k^{12} \pm 1 - m_j + m_i$

$k \in [K_{21}]$

$\alpha_k^{21} \pm 1 - m_j + m_i$
$\beta_k^{21} \pm 1 + m_j - m_i$

$k \in [K_{22}]$

$\alpha_k^{22} \mp 1 - m_j - m_i$
$\beta_k^{22} \mp 1 + m_j + m_i$

$k \in [K_{20}]$

$\alpha_k^{20} - m_j$
$\beta_k^{20} + m_j$

$k \in [K_{01}]$

$\alpha_k^{01} + m_i$
$\beta_k^{01} - m_i$

$k \in [K_{10}]$

$\alpha_k^{10} + m_j$
$\beta_k^{10} - m_j$

$k \in [K_{02}]$

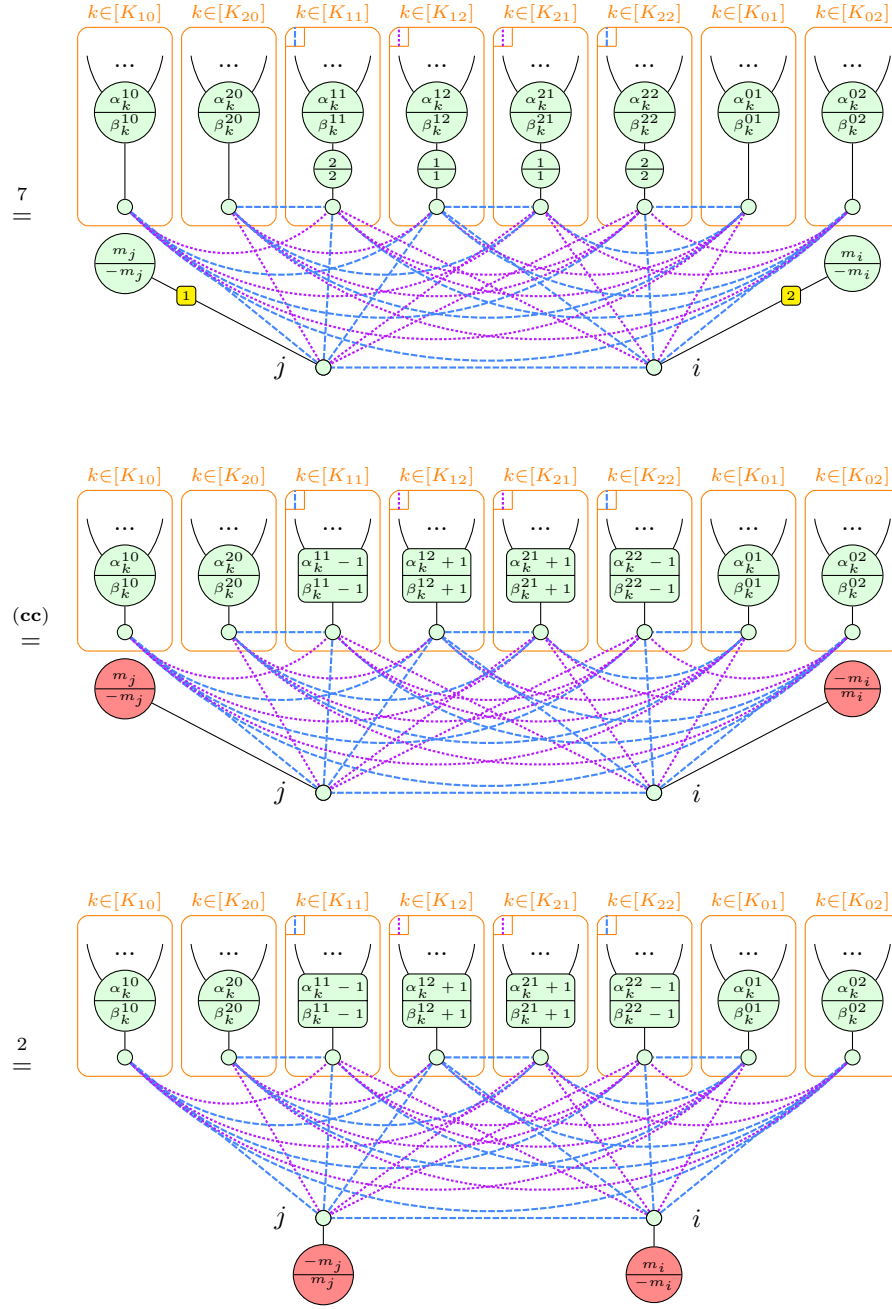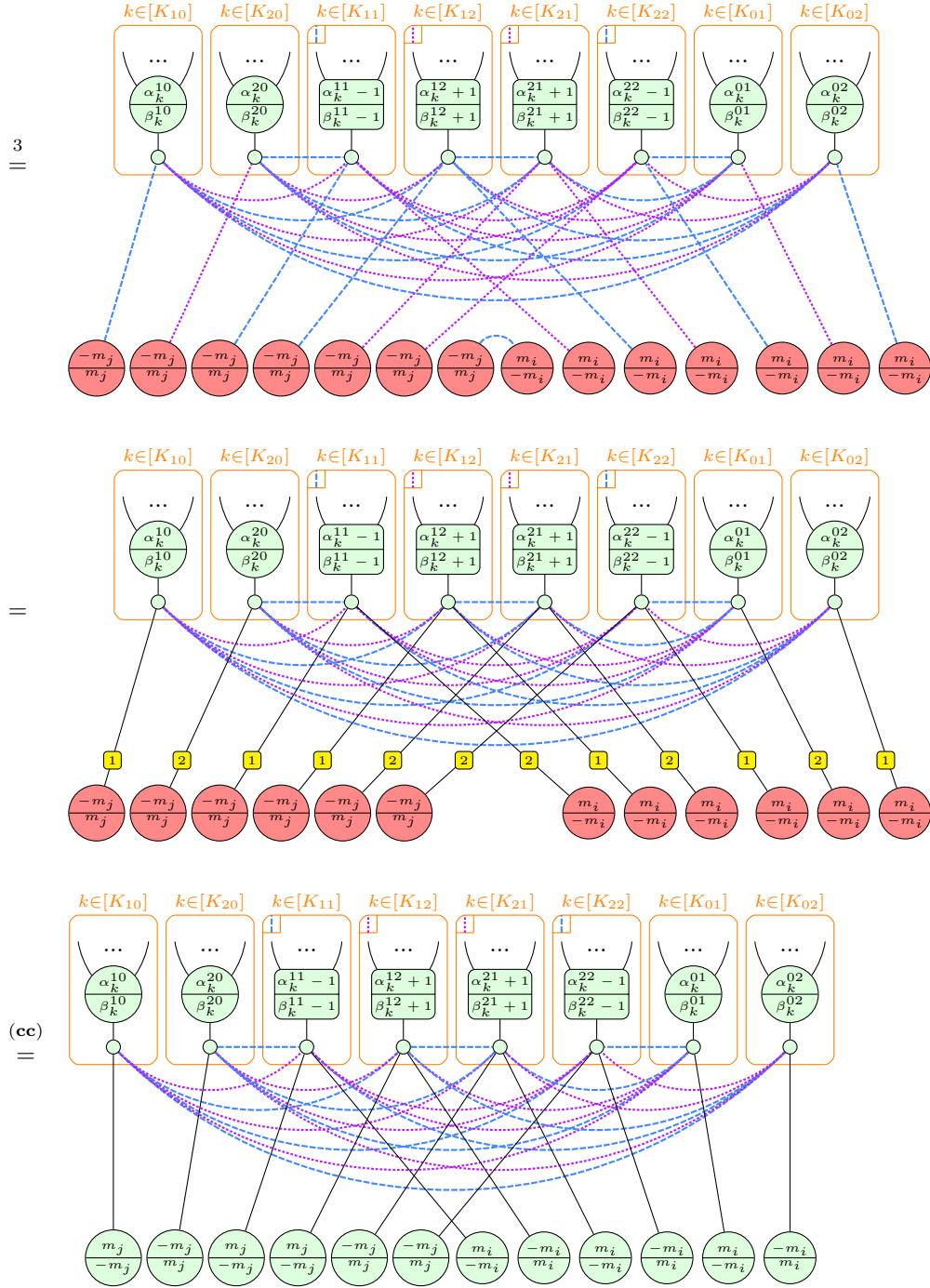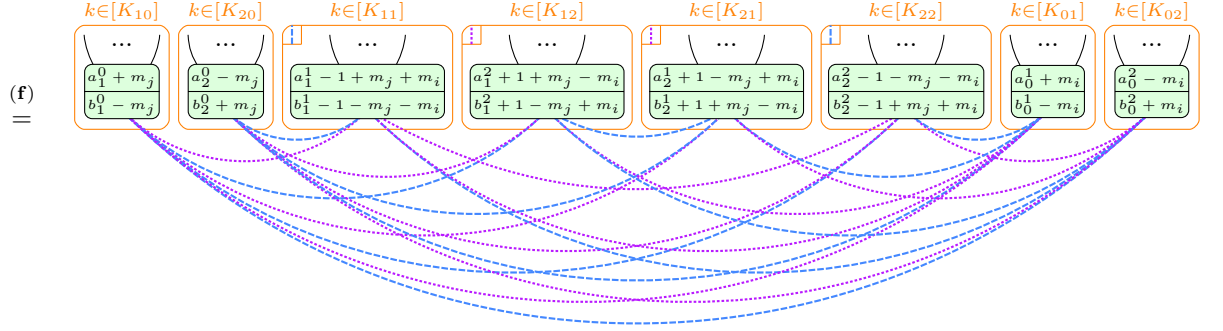$\alpha_k^{02} - m_i$
$\beta_k^{02} + m_i$
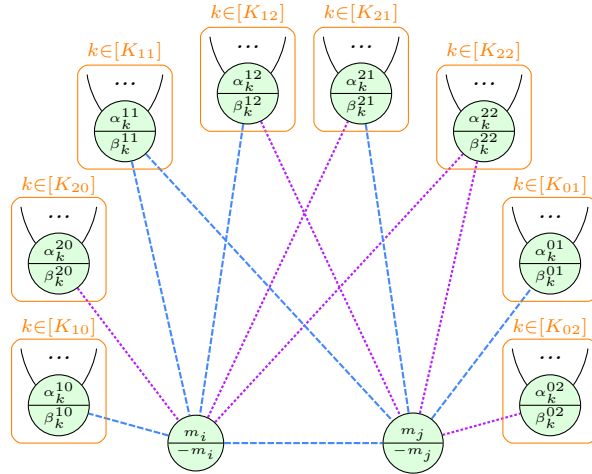
The case $w = 2$ differs only as follows: in the first diagram (the left hand side of the equation), the edge ij is purple (by definition), while in the lower diagram (the right hand side of the equation), a $\pm 2 = \mp 1$ will replace all occurences of ± 1, and the roles of purple and blue will be swapped throughout.

Proof. We show the case where $w_{ij} =: w = 1$, with the case $w = 2$ being completely analogous. We can choose either a proper 1-pivot or a proper 2-pivot; both give the same result. Here we only show the former:

$k \in [K_{10}]$ $\quad$ $k \in [K_{20}]$ $\quad$ $k \in [K_{11}]$ $\quad$ $k \in [K_{12}]$ $\quad$ $k \in [K_{21}]$ $\quad$ $k \in [K_{22}]$ $\quad$ $k \in [K_{01}]$ $\quad$ $k \in [K_{02}]$

α_k^{10} $\quad$ α_k^{20} $\quad$ α_k^{11} $\quad$ α_k^{12} $\quad$ α_k^{21} $\quad$ α_k^{22} $\quad$ α_k^{01} $\quad$ α_k^{02}
β_k^{10} $\quad$ β_k^{20} $\quad$ β_k^{11} $\quad$ β_k^{12} $\quad$ β_k^{21} $\quad$ β_k^{22} $\quad$ β_k^{01} $\quad$ β_k^{02}

i $\quad \dfrac{m_i}{-m_i} \quad$ $\quad \dfrac{m_j}{-m_j} \quad j$

$(\mathbf{f}) =$

$k \in [K_{10}]$ $\quad$ $k \in [K_{20}]$ $\quad$ $k \in [K_{11}]$ $\quad$ $k \in [K_{12}]$ $\quad$ $k \in [K_{21}]$ $\quad$ $k \in [K_{22}]$ $\quad$ $k \in [K_{01}]$ $\quad$ $k \in [K_{02}]$

α_k^{10} $\quad$ α_k^{20} $\quad$ α_k^{11} $\quad$ α_k^{12} $\quad$ α_k^{21} $\quad$ α_k^{22} $\quad$ α_k^{01} $\quad$ α_k^{02}
β_k^{10} $\quad$ β_k^{20} $\quad$ β_k^{11} $\quad$ β_k^{12} $\quad$ β_k^{21} $\quad$ β_k^{22} $\quad$ β_k^{01} $\quad$ β_k^{02}

$\dfrac{m_i}{-m_i}$ $\qquad\qquad\qquad\qquad\qquad\qquad\qquad$ $\dfrac{m_j}{-m_j}$

i $\qquad\qquad\qquad\qquad\qquad$ j

$k \in [K_{10}]$ $k \in [K_{20}]$ $k \in [K_{11}]$ $k \in [K_{12}]$ $k \in [K_{21}]$ $k \in [K_{22}]$ $k \in [K_{01}]$ $k \in [K_{02}]$

(**f**) =

E $\pm$-Boxes in the ZX Calculus

We close by proving that the $\pm$-boxes in (17) correspond to stabilizer ZX-diagrams, while the qutrit X-box in (20) does not.

Proposition 3. *The following equalities hold up to a scalar under the standard interpretation:*

$$
\left[\!\!\left[\; \boxed{\pm} \;\right]\!\!\right]_{d=2} \simeq \left[\!\!\left[\; \pm\tfrac{\pi}{2} \;\right]\!\!\right] , \qquad
\left[\!\!\left[\; \boxed{\pm} \;\right]\!\!\right]_{d=3} \simeq \left[\!\!\left[\; \begin{smallmatrix}\pm 1 \\ \pm 1\end{smallmatrix} \;\right]\!\!\right] , \qquad
\left[\!\!\left[\; \boxed{\pm} \;\right]\!\!\right]_{d=4} \simeq \left[\!\!\left[\; \pi - \square - \pi \;\right]\!\!\right]
$$
$$(46)$$

Proof. Recalling $\omega = e^{i\frac{2\pi}{3}}$, the standard interpretations of phase gates in matrix form are:

$$
\left[\!\!\left[\; \alpha \;\right]\!\!\right] = \begin{pmatrix} 1 & 0 \\ 0 & e^{i\alpha} \end{pmatrix} , \qquad
\left[\!\!\left[\; \alpha \;\right]\!\!\right] = \frac{1}{2}\begin{pmatrix} 1+e^{i\alpha} & 1-e^{i\alpha} \\ 1-e^{i\alpha} & 1+e^{i\alpha} \end{pmatrix} , \qquad
\left[\!\!\left[\; \begin{smallmatrix}\alpha\\\beta\end{smallmatrix} \;\right]\!\!\right] = \begin{pmatrix} 1 & 0 & 0 \\ 0 & e^{i\alpha} & 0 \\ 0 & 0 & e^{i\beta} \end{pmatrix}
$$

$$
\left[\!\!\left[\; \begin{smallmatrix}\alpha\\\beta\end{smallmatrix} \;\right]\!\!\right] = \frac{1}{3}\begin{pmatrix}
1+e^{i\alpha}+e^{i\beta} & 1+\bar\omega e^{i\alpha}+\omega e^{i\beta} & 1+\omega e^{i\alpha}+\bar\omega e^{i\beta} \\
1+\omega e^{i\alpha}+\bar\omega e^{i\beta} & 1+e^{i\alpha}+e^{i\beta} & 1+\bar\omega e^{i\alpha}+\omega e^{i\beta} \\
1+\bar\omega e^{i\alpha}+\omega e^{i\beta} & 1+\omega e^{i\alpha}+\bar\omega e^{i\beta} & 1+e^{i\alpha}+e^{i\beta}
\end{pmatrix}
$$

So in the simplest case $d=2$ it is fairly straightforward to see that:

$$
\left[\!\!\left[\; \pm\tfrac{\pi}{2} \;\right]\!\!\right] \;=\; \frac{1}{2}\begin{pmatrix} 1\pm i & 1\mp i \\ 1\mp i & 1\pm i \end{pmatrix} \;=\; \frac{\sqrt{2}}{2} e^{\mp i\frac{\pi}{4}}\begin{pmatrix} \pm i & 1 \\ 1 & \pm i \end{pmatrix} \;=\; \frac{\sqrt{2}}{2} e^{\mp i\frac{\pi}{4}}\left[\!\!\left[\; \boxed{\pm} \;\right]\!\!\right]_{d=2}
$$
$$(47)$$

The next case $d = 3$ is proved similarly:

$$
\left[\!\left[\; \begin{smallmatrix} \pm 1 \\ \pm 1 \end{smallmatrix} \;\right]\!\right] = \frac{1}{3} \begin{pmatrix} 1 + e^{\pm i \frac{2\pi}{3}} + e^{\pm i \frac{2\pi}{3}} & 1 + \bar\omega e^{\pm i \frac{2\pi}{3}} + \omega e^{\pm i \frac{2\pi}{3}} & 1 + \omega e^{\pm i \frac{2\pi}{3}} + \bar\omega e^{\pm i \frac{2\pi}{3}} \\ 1 + \omega e^{\pm i \frac{2\pi}{3}} + \bar\omega e^{\pm i \frac{2\pi}{3}} & 1 + e^{\pm i \frac{2\pi}{3}} + e^{\pm i \frac{2\pi}{3}} & 1 + \bar\omega e^{\pm i \frac{2\pi}{3}} + \omega e^{\pm i \frac{2\pi}{3}} \\ 1 + \bar\omega e^{\pm i \frac{2\pi}{3}} + \omega e^{\pm i \frac{2\pi}{3}} & 1 + \omega e^{\pm i \frac{2\pi}{3}} + \bar\omega e^{\pm i \frac{2\pi}{3}} & 1 + e^{\pm i \frac{2\pi}{3}} + e^{\pm i \frac{2\pi}{3}} \end{pmatrix}
$$

$$
= \frac{1}{3} \begin{pmatrix} \sqrt{3} e^{\pm i \frac{\pi}{2}} & \sqrt{3} e^{\mp i \frac{\pi}{6}} & \sqrt{3} e^{\mp i \frac{\pi}{6}} \\ \sqrt{3} e^{\mp i \frac{\pi}{6}} & \sqrt{3} e^{\pm i \frac{\pi}{2}} & \sqrt{3} e^{\mp i \frac{\pi}{6}} \\ \sqrt{3} e^{\mp i \frac{\pi}{6}} & \sqrt{3} e^{\mp i \frac{\pi}{6}} & \sqrt{3} e^{\pm i \frac{\pi}{2}} \end{pmatrix}
$$

$$
= \frac{\sqrt{3}}{3} e^{\mp i \frac{\pi}{6}} \begin{pmatrix} e^{\pm i \frac{2\pi}{3}} & 1 & 1 \\ 1 & e^{\pm i \frac{2\pi}{3}} & 1 \\ 1 & 1 & e^{\pm i \frac{2\pi}{3}} \end{pmatrix}
$$

$$
= \frac{\sqrt{3}}{3} e^{\mp i \frac{\pi}{6}} \left[\!\left[\; \boxed{\pm} \;\right]\!\right]_{d=3}
$$

$$\tag{48}$$

For the other qubit case $d = 4$ we first note:

$$
\left[\!\left[\; \square \;\right]\!\right] = \left[\!\left[\; \begin{smallmatrix} \frac{\pi}{2} \\ \frac{\pi}{2} \\ \frac{\pi}{2} \end{smallmatrix} \;\right]\!\right] = \left[\!\left[\; \frac{\pi}{2} \;\right]\!\right] \left[\!\left[\; \frac{\pi}{2} \;\right]\!\right] \left[\!\left[\; \frac{\pi}{2} \;\right]\!\right] = \frac{1}{2\sqrt{2}} \begin{pmatrix} 1 & 1 \\ 1 & -1 \end{pmatrix} \tag{49}
$$

Then using the standard interpretation for spiders as in (1), we decompose the diagram in such a way that we can apply the standard interpretation:

$$
\left[\!\left[\; \pi - \square - \pi \;\right]\!\right] = \left[\!\left[\; \text{(diagram)} \;\right]\!\right]
$$

$$
= \left(\left[\!\left[\; | \;\right]\!\right] \otimes \left[\!\left[\; \pi \;\right]\!\right] \right) \left(\left[\!\left[\; | \;\right]\!\right] \otimes \left[\!\left[\; \square \;\right]\!\right] \otimes \left[\!\left[\; | \;\right]\!\right] \right) \left(\left[\!\left[\; \pi \;\right]\!\right] \otimes \left[\!\left[\; | | \;\right]\!\right] \right)
$$

$$
= \frac{\sqrt{2}}{8} \begin{pmatrix} -1 & 1 & 1 & 1 \\ 1 & -1 & 1 & 1 \\ 1 & 1 & -1 & 1 \\ 1 & 1 & 1 & -1 \end{pmatrix}
$$

$$
= \frac{\sqrt{2}}{8} \left[\!\left[\; \boxed{\pm} \;\right]\!\right]_{d=4}
$$

$$\square$$

Now we prove the qutrit X-box is not a stabilizer diagram. The following lemma is required:

Lemma 6. *Every stabilizer state is equivalent to one of the following 12 diagrams:*
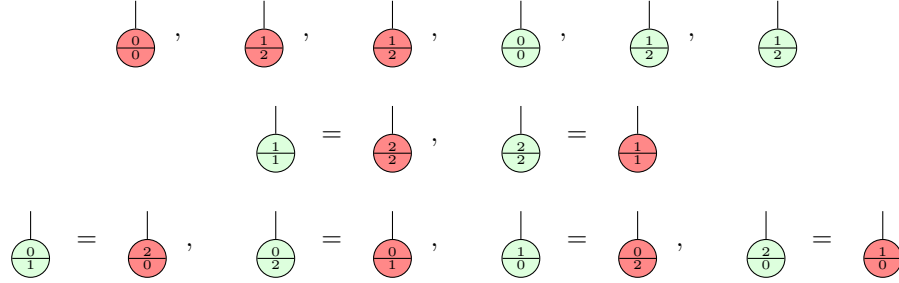
Proof. We can use our elimination rules to prove this. A stabilizer state is a diagram with no inputs and one output, in which every phase component is a multiple of $\frac{2\pi}{3}$. After putting it in graph-like form (via Proposition 1), all but one spider will be interior. We'll call the non-interior one the *boundary* spider. Our elimination rules say we can remove all interior $\mathcal{P}$- and $\mathcal{N}$-spiders, plus all pairs of connected interior $\mathcal{M}$-spiders. So applying these rules until we can do so no more, we have two cases. The easiest case is where end up with just the single boundary spider, which must have no inputs and one output. In the other case we get a single $\mathcal{M}$-spider connected to a boundary spider. The $\mathcal{M}$-spider can have no other legs, and the boundary spider must have exactly one other leg, which is the output of the overall diagram:

(50)

In the first case, we're done. In the second case, we need only note:

$\square$

Proposition 4. *The qutrit X-box defined below is not a stabilizer diagram:*

$$\left[\!\!\left[\; \boxed{X} \;\right]\!\!\right] \;=\; \sum_{i,j=0}^{d-1}(1-\delta_{ij})\,|i\rangle\langle j| \;=\; \begin{pmatrix} 0 & 1 & 1 \\ 1 & 0 & 1 \\ 1 & 1 & 0 \end{pmatrix}$$

Proof. Stabilizer diagrams are closed under composition (they form a group). Hence if the X-box is stabilizer, it must send the phaseless red spider state to a stabilizer state. This has matrix:

$$
\left[\!\!\left[\; \boxed{X} \; \right]\!\!\right] \;=\; \left[\!\!\left[\; \boxed{X} \; \right]\!\!\right]\left[\!\!\left[\; \bullet \; \right]\!\!\right] \;=\; \begin{pmatrix} 0 & 1 & 1 \\ 1 & 0 & 1 \\ 1 & 1 & 0 \end{pmatrix}\begin{pmatrix} 1 \\ 0 \\ 0 \end{pmatrix} \;=\; \begin{pmatrix} 0 \\ 1 \\ 1 \end{pmatrix}
$$

But, up to a scalar, this is not equal to any of the 12 stabilizer states above:

$$
\left[\!\!\left[\; \bullet \; \right]\!\!\right] = \begin{pmatrix} 1 \\ 0 \\ 0 \end{pmatrix}, \quad \left[\!\!\left[\; \tfrac{1}{2} \; \right]\!\!\right] = \begin{pmatrix} 0 \\ 1 \\ 0 \end{pmatrix}, \quad \left[\!\!\left[\; \tfrac{2}{1} \; \right]\!\!\right] = \begin{pmatrix} 0 \\ 0 \\ 1 \end{pmatrix}, \quad \left[\!\!\left[\; \tfrac{a}{b} \; \right]\!\!\right] = \begin{pmatrix} 1 \\ \omega^a \\ \omega^b \end{pmatrix}
$$

$\square$